

### **ScienceDirect**



IFAC PapersOnLine 54-4 (2021) 112-117

# Complementary Stability of Markovian Systems: Series Elastic Actuators and Human-Robot Interaction \*

Andres L. Jutinico \* Oscar Flórez-cediel \* Adriano A. G. Siqueira \*\*

\* Universidad Distrital Francisco José de Caldas, Bogotá, Colombia (e-mail:{aljutinicoa, odflorez}@udistrital.edu.co). \*\* University of São Paulo, São Carlos, Brazil (e-mail: siqueira@sc.usp.br).

Abstract: This paper presents an extension of the complementary stability analysis for discrete-time Markovian systems applied in interaction control. The control strategy considers an internal loop force control for Series Elastic Actuators based on the Robust Regulator for Discrete-time Markov Jump Linear systems and extern loop impedance control to regulate the interaction between the human and robot. Two examples show the complementary stability analysis of the human-robot interaction system, where is regarded as different values of the virtual impedances, different levels for the robustness of the force control, uncertainties, and abrupt changes for human parameters. Simulation results show the capacity of control strategy to deal with active interaction models, where the Mean Square Stability guarantees safe for the user. Additionally, from results it is understood the transmissibility of impedance achieved is a consequence of the robust performance given by the force controller.

Copyright © 2021 The Authors. This is an open access article under the CC BY-NC-ND license (https://creativecommons.org/licenses/by-nc-nd/4.0/)

Keywords: Markovian jump linear systems, Robotic rehabilitation, Robust control, Complementary stability.

#### 1. INTRODUCTION

For the past three decades, researchers of the roboticrehabilitation area have developed platforms, orthosis, and exoskeletons for ankle rehabilitation to promote the active participation of patients in the rehabilitation process. In this context, where machines and humans are coupled to solve a specific work, the technology of control, actuators, and sensors for interaction robots must warrant safe, and precision (Ajoudani et al., 2018). Series Elastic Actuators (SEA's) are an example of technology advances for Human-Robot Interaction. These mechatronic devices allow safety in the interaction to use a spring located between the environment and the robot (Pratt and Williamson, 1995). Robots based on series elastic actuators require an inner force loop control, which can be sensitive to human variations. The change of behavior of human impedance during the gait is related to higher ankle stiffness for stance and low for swing phase (Lee et al., 2016). These abrupt changes of parameters can be treated by Markovian models with bounded uncertainties (Jutinico et al., 2017; Escalante et al., 2021). Nevertheless, the complementary stability of the human and the rehabilitation robot must be guaranteed to bring safety for users (Buerger and Hogan, 2007). Therefore, a suitable strategy to give stability is the impedance control (IC) that modifies the robot torque by virtual stiffness and damping (Hogan, 1985). However, in SEA's based devices, this stability depends on both impedance control and force control. Since the interaction system can be modeled by discrete-time Markov jump linear systems, the complementary stability must be analyzed via spectral radius (Costa et al., 2005). In this paper, we analyze the complementary stability of Markovian systems. We pay special attention in SEA's based robots and make a proof of concept using the IC with the Linear Quadratic Regulator (LQR-DMJLS) and the Robust Regulator for Discrete-time Markov Jump Linear Systems (RR-DMJLS).

The rest of this paper is organized as follows: Section 2 introduce the interaction control for DMJLS; Section 3 is the complementary stability for DMJLS; in Section 4 we show the stability analysis; Section 5 present the proof of concept; in Section 6 are explained the results and in Section 7 the conclusions.

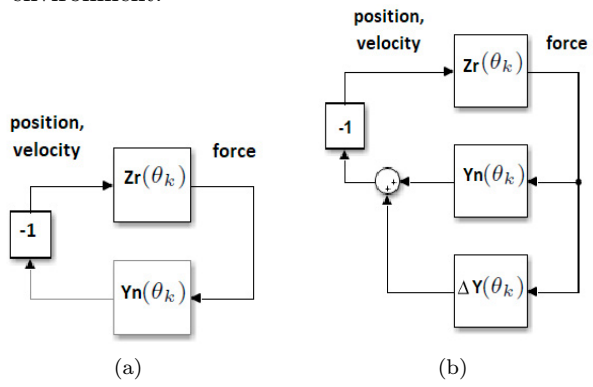
#### 2. INTERACTION CONTROL FOR DMJLS

The interaction systems usually are represented by port functions to describe coupled physical joints. The above allows illustrating systems with block diagrams by conjugate power variables without making assumptions about loading (Buerger and Hogan, 2007). Fig. 1 (a) shows a block diagram representing the interaction between a robot and an unknown environment. The robot is denoted by an impedance  $Z_r$  and the environment by an admittance  $Y_n$ . In this context, the system stability depends on both robot and the environment since the characteristic system equation is given by  $(1 + Z_r Y_n)$ . In contrast,

 $<sup>^\</sup>star$  This work is supported by Universidad Distrital Francisco José de Caldas under grant 2-5-617-20.

the system performance depends on the robot  $Z_r$ , and a form to quantify this performance is through impedance transmissibility from the robot to the environment. Notice

Fig. 1. Robot interacting with an uncertain and Markovian environment.



that the robot  $Z_r$  actually is the set of devices to make an automatic action, including actuators, sensors, and mechanisms. For instance, in HRI systems based on SEA, explicit force control is necessary. This control can be related to the model of the system to obtain optimal performance. Besides, both robots as the environment can be modeled as Markov jump linear systems. When the system is subject to abrupt changes, or there is random model variability, the system can be modeled from multimodal linear systems subject to jumps. In this case,  $Z_r$  and  $Y_n$  depend on the jump parameter  $\theta_k$ .

#### 2.1 Impedance Control

The impedance control considered in this paper is defined as follows,

$$\tau_k^d = B_v(\omega_{lk}^d - \omega_{lk}) + K_v(\phi_{lk}^d - \phi_{lk}) + K_v\varepsilon\phi_{lk}^d, \tag{1}$$

where  $\tau_k^d$  is the desired torque,  $\phi_{lk}^d$  is the desired trajectory of the load, and  $\omega_{lk}^d$  corresponds to the desired velocity.  $K_v$  and  $B_v$  are the desired stiffness and damping respectively, which are responsible for control interaction with the environment, and  $K_v \varepsilon \phi_{lk}^d$  is a feed-forward term that reduces the overshoot in the angle through the tuning parameter  $\varepsilon$ .

#### 2.2 Linear Quadratic Regulator for DMJLS

Consider the nominal DMJLS (2), which represents a coupled system between a human and a robot. Notice that robot  $Z_r(\theta_k)$  showed in Fig. 1 (a), it is including an IC and a feedback force control given by the LQR-DMJLS. Where  $x_k \in \mathbb{R}^n$  is the state vector,  $u_k \in \mathbb{R}^m$  the control input,  $F_{i,k} \in \mathbb{R}^{n \times n}$  and  $B_{i,k} \in \mathbb{R}^{n \times m}$  are parametric matrices, and the jump parameter  $\theta_k = i$ .

$$x_{k+1} = F_{i,k}x_k + B_{i,k}u_k, \quad k = 0, \dots, N-1.$$
 (2)

The aim of the control is to find the control sequence  $u_k$  that minimize the expected cost function given in (3) subject to model (2). The transition probability matrix  $p_{i,j}$  and the appropriate weighting matrices  $P_{i,k} \succ 0$ ,  $Q_{i,k} \succ 0$ ,  $R_{i,k} \succ 0$  allow obtain a optimal control law  $u_k^* = K_{i,k}x_k$  and the control vector  $K_{i,k}$  by the recursive equations (4) to (6), see Costa et al. (2005).

$$J = x_{k+1}^T \Psi_{i,k+1} x_{k+1} + \sum_{k=0}^{N-1} (x_k^T Q_{i,k} x_k + u_k^T R_{i,k} u_k), \quad (3)$$

$$\Psi_{i,k+1} = \sum_{j=1}^{s} P_{j,k+1} p_{ij}, \tag{4}$$

$$P_{i,k} = F_{i,k}^{T} (\Psi_{i,k+1} - \Psi_{i,k+1} B_{i,k} (R_{i,k} + B_{i,k}^{T} \Psi_{i,k+1} B_{i,k})^{-1} B_{i,k}^{T} \Psi_{i,k+1}) F_{i,k} + Q_{i,k},$$
(5)

$$K_{i,k} = -(R_{i,k} + B_{i,k}^T \Psi_{i,k+1} B_{i,k})^{-1} B_{i,k}^T \Psi_{i,k+1} F_{i,k}.$$
 (6)

#### 3. THE COMPLEMENTARY STABILITY FOR DMJLS

According to Buerger and Hogan (2007), the HRI problem can treat like a robust control problem considering the complementary stability. In this context, Fig. 1 (b) shows the robot by an impedance  $Z_r$  connecting with the environment, which in this case is the human, and is regarded as a simplified nominal model  $Y_n$  with boundary uncertainties  $\Delta Y$ . These uncertainties concerning the human parameters always are bounded, e.g., mass and height can vary between individuals but always into a range. Notice that using a Markovian robust regulator in the robot, the effect of these additive uncertainties can be avoided. Therefore, the interaction problem is deal with by an impedance control, and the Markovian control will be tuning both to passive and active operation modes.

#### 3.1 Markovian Robust Regulator

Consider the uncertain DMJLS (7), which represents a complementary system between a human and a robot, with  $Z_r(\theta_k)$ ,  $Y_n(\theta_k)$ , and  $\Delta Y(\theta_k)$ , as shown in Fig. 1 (b). The robot includes an IC and a feedback force control given by the RR-DMJLS.

$$x_{k+1} = (F_{i,k} + \delta F_{i,k})x_k + (B_{i,k} + \delta B_{i,k})u_k,$$
 (7)

for all k=0,...,N-1. The nominal matrices of the Markovian model are  $F_{i,k}$  and  $B_{i,k}$ . Uncertain matrices  $\delta F_{i,k}$  and  $\delta B_{i,k}$  are defined as follows:

$$\left[\delta F_{i,k} \ \delta B_{i,k}\right] = H_{i,k} \Delta_{i,k} \left[E_{F_{i,k}} \ E_{B_{i,k}}\right], \tag{8}$$

where  $H_{i,k} \in \mathbb{R}^{n \times q}$ ,  $E_{F_{i,k}} \in \mathbb{R}^{l \times n}$  and  $E_{B_{i,k}} \in \mathbb{R}^{l \times m}$  are known matrices, and  $\Delta_{i,k} \in \mathbb{R}^{q \times l}$  is a contraction such that  $\|\Delta_{i,k}\| \leq 1$ .

The RR-DMJLS we consider in this paper was reported in (Cerri and Terra, 2017). It is developed based on the solution of the following optimization problem:

$$\min_{x_{k+1}, u_k} \max_{\delta F_{i,k}, \delta B_{i,k}} \{ \mathcal{J}_k^{\mu} \}, \tag{9}$$

$$\mathcal{J}_{k}^{\mu} = \begin{bmatrix} x_{k+1} \\ u_{k} \end{bmatrix}^{T} \begin{bmatrix} \Psi_{i,k+1} & 0 \\ 0 & R_{i,k} \end{bmatrix} \begin{bmatrix} x_{k+1} \\ u_{k} \end{bmatrix} + \\
\begin{cases} \begin{bmatrix} 0 & 0 \\ I & -B_{i,k}^{\delta} \end{bmatrix} \begin{bmatrix} x_{k+1} \\ u_{k} \end{bmatrix} - \begin{bmatrix} -I \\ F_{i,k}^{\delta} \end{bmatrix} x_{k} \end{cases}^{T} \begin{bmatrix} Q_{i,k} & 0 \\ 0 & \mu I \end{bmatrix} \{ \bullet \}. 
\end{cases} (10)$$

The RR-DMJLS aims to minimize the state vector  $x_{k+1}$  and the control input  $u_k$  against the maximization of

parametric uncertainties  $\delta F_{i,k}$  and  $\delta B_{i,k}$ . In (10),  $\Psi_{j,k+1} = \sum_{j=1}^{s} P_{j,k+1} p_{ij}$ , and  $P_{j,k} \succ 0$ ,  $Q_{j,k} \succ 0$ , and  $R_{i,k} \succ 0$  are weighting matrices. Control vector  $K_{i,k}$ , closed loop matrix  $L_{i,k}$ , optimal states of the closed-loop system  $x_{k+1}^*$  and control action  $u_k^*$  are computed by the algorithm (12) (where I is an identity matrix of appropriate dimension). If all states of the system are available and  $\mu \rightarrow +\infty$ ,  $W_{i,k} \rightarrow 0$ , the system robustness is obtained, and

$$\begin{cases}
L_{i,k} = F_{i,k} + B_{i,k} K_{i,k} \\
E_{F_{i,k}} + E_{B_{i,k}} K_{i,k} = 0.
\end{cases}$$
(11)

## Robust Regulator for DMJLS Initial Conditions:

Set  $x_0, \theta_0, \mathbb{P}, P_i(N) > 0, \forall i \in \{1, ..., s\}.$ 

**Step 1:** (Backward). Calculate, for all k = N - 1, ..., 0,

$$\begin{bmatrix} L_{i,k} \\ K_{i,k} \\ P_{c,i,k} \end{bmatrix} = \begin{bmatrix} 0 & 0 & 0 & I & 0 \\ 0 & 0 & 0 & 0 & I \\ 0 & 0 & -I & \hat{F}_{i,k} & 0 & 0 \end{bmatrix} \times$$

$$\begin{bmatrix} \Psi_{i,k+1}^{-1} & 0 & 0 & 0 & I & 0 \\ 0 & R_{i,k}^{-1} & 0 & 0 & 0 & I \\ 0 & 0 & Q_{i,k}^{-1} & 0 & 0 & 0 \\ 0 & 0 & 0 & \mathcal{W}_{i,k} & \hat{I} - \hat{B}_{i,k} \\ I & 0 & 0 & \hat{I}^T & 0 & 0 \\ 0 & I & 0 & -\hat{B}_{i,k}^T & 0 & 0 \end{bmatrix}^{-1} \begin{bmatrix} 0 \\ 0 \\ -I \\ \hat{F}_{i,k} \\ 0 \\ 0 \end{bmatrix},$$

$$\Psi_{i,k+1} = \sum_{j=1}^{s} P_{j,k+1} p_{ij}, \quad \hat{\lambda}_{i,k} > \|\mu H_{i,k}^{T} H_{i,k}\|,$$

$$\hat{F}_{i,k} = \begin{bmatrix} F_{i,k} \\ E_{F_{i,k}} \end{bmatrix}, \quad \hat{B}_{i,k} = \begin{bmatrix} B_{i,k} \\ E_{B_{i,k}} \end{bmatrix}, \quad \hat{I} = \begin{bmatrix} I \\ 0 \end{bmatrix},$$

$$\mathcal{W}_{i,k} = \begin{bmatrix} \mu^{-1}I - \hat{\lambda}_{i,k}^{-1}H_{i,k}H_{i,k}^T & 0\\ 0 & \hat{\lambda}_{i,k}^{-1}I \end{bmatrix},$$

**Step 2:** (Forward). Obtain, for each k = 0, ..., N-1,

$$\begin{bmatrix} x_{k+1}^* \\ u_k^* \end{bmatrix} = \begin{bmatrix} L_{i,k} \\ K_{i,k} \end{bmatrix} x_k^*. \tag{12}$$

#### 4. STABILITY ANALYSIS

This section is the stability analysis of the HRI case with uncertainties and an actuator to guarantee the robot's desired torque, for instance, with SEAs. In (13) and (14), the human and robot are considered in a complementary model, where matrices  $F_{i,k}$  and  $B_{i,k}$  include nominal parameters both human and robot. The bounded uncertain parameters are defined by  $\delta F_{i,k}$  and  $\delta B_{i,k}$ . Besides, the model assumes an integral action to correct the torque error, and that one of the system states is the actuator torque, as follow:

$$x_{k+1} = (F_{i,k} + \delta F_{i,k})x_k + (B_{i,k} + \delta B_{i,k})u_k + B_{r_k}\tau_k^d,$$
 (13)

$$z_k = C_2 x_k + D_2 u_k, (14)$$

where, velocity and trajectory of system are defined by a linear array of equations with  $z_k = [\omega_{ik} \ \phi_{ik}]^T$ , and  $u_k = K_{i,k}x_k$ . According to the equations (1), (11) and (13) then,

$$x_{k+1} = [F_{i,k} + B_{i,k}K_{i,k}] x_k + B_{r_k} \left[ B_v(\omega_{ik}^d - \omega_{ik}) + K_v(\phi_{ik}^d - \phi_{ik}) + K_v\varepsilon\phi_{ik}^d \right],$$
(15)

notice that,  $z_k = [C_2 + D_2 K_{i,k}] x_k$ , thus, after some algebraic manipulations the following closed-loop equation for impedance control is obtained:

$$x_{k+1} = \left[ \mathbb{A}_{1i,k} + \mathbb{A}_{2i,k} \right] x_k + B_{r_k} \left[ B_v \left( 1 + \varepsilon \right) K_v \right] \begin{bmatrix} \omega_{lk}^d \\ \phi_{lk}^d \end{bmatrix}, \tag{16}$$

with its auxiliary matrices defined by,

$$\mathbb{A}_{1i,k} = [F_{i,k} + B_{i,k} K_{i,k}], \qquad (17)$$

$$\mathbb{A}_{2i,k} = B_{r_k} \left[ -B_v - K_v \right] \left[ C_2 + D_2 K_{i,k} \right]. \tag{18}$$

Thus, the Mean Square Stability (MSS) is given by,

$$r_{\sigma}(\mathbb{A}_{1i,k} + \mathbb{A}_{2i,k}) \le 1,\tag{19}$$

where,  $r_{\sigma}(\mathbb{A}_{1i,k} + \mathbb{A}_{2i,k})$  is the spectral radius (for more details see Costa et al. (2005)).

#### 5. PROOF OF CONCEPT

This section is elaborate a proof of concept to shows the uncertainties effect over markovian interaction system. It is considered the System Robotic Platform for Ankle Rehabilitation (SRPAR) in interaction with a user (Jutinico et al., 2017). This robot count with a SEA. Therefore an explicit force control is necessary. The force/torque control considered is Markovian since this platform deals with varying and uncertain human nature. The proof of concept consists of validating the Mean Square Stability with the impedance control and an LQR-DMJLS or an RR-DMJLS force controller. Following is introduced the robot, the force control topology, and design parameters for the Markovian controls.

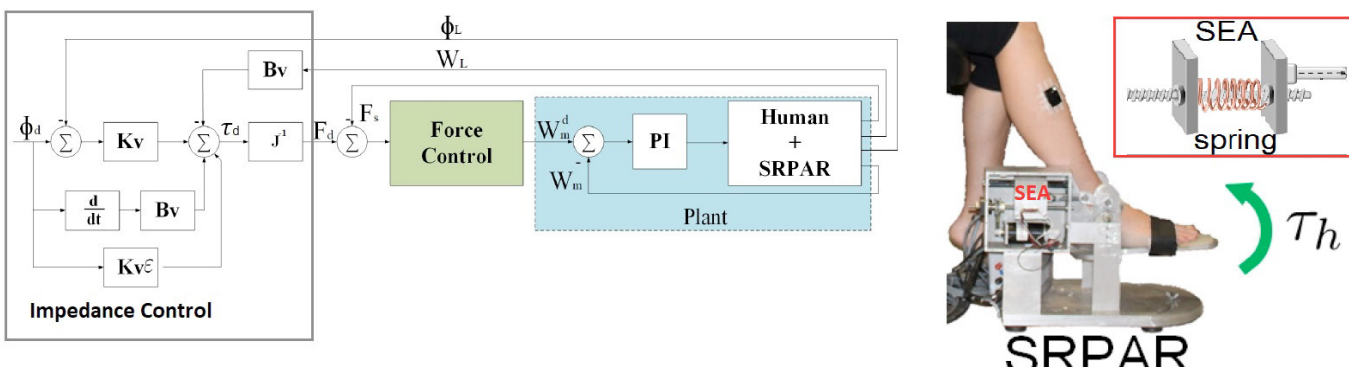
#### 5.1 The robot

The SRPAR aims to perform controlled movements of the ankle for therapeutic purposes. Fig. 2 shows the overall configuration of the interaction control. The plant is the complementary system of human parameters and the SRPAR. Notice that the robot use inners loops of current and velocity. This picture also is shown the force and impedance control when the robot is coupled with the human.

The dynamical model of the SRPAR has been studied in (Jutinico et al., 2017, 2018; Escalante et al., 2021) and is shows in (20) and (21). The state vector  $x_a$  includes the angular position of the load  $\phi_l$ , the spring force  $F_s$ , and its first derivate respect to time  $\dot{F}_s$ . The angular velocity of the motor  $\omega_m$  is the control input of the system. The human torque  $\tau_h$  and the angular position of the motor  $\phi_m$  are input disturbances.

The output load consists of a 4-link mechanism coupled to the foot. The angular movement is mapped to linear displacement by the Jacobian constant  $\mathcal{J}$ . We used a second-order model (stiffness, damping, and inertia) to represent

Fig. 2. Overall configuration of the interaction control.



(20)

ankle dynamics. The output mechanical impedance describing the interaction between the ankle and platform is characterized by the equivalent inertia  $J_l = J_{plat} + J_h$ , damping  $C_l = C_{plat} + C_h$ , and stiffness  $K_h$ , with subscripts  $p_{lat}$  for platform and h for human.

$$\underbrace{\begin{bmatrix} \ddot{F}_s(t) \\ \dot{F}_s(t) \\ \dot{\phi}_l(t) \end{bmatrix}}_{\dot{x}_a(t)} = \underbrace{\begin{bmatrix} \frac{K_s \mathcal{J}}{J_l(t)} \\ 0 \\ 0 \end{bmatrix}}_{\mathcal{G}_s^s(\theta_k)} \tau_h(t) + \underbrace{\begin{bmatrix} \frac{K_l(t)K_s}{\rho N_p J_l(t)} \\ 0 \\ 0 \end{bmatrix}}_{\mathcal{G}_s^s(\theta_k)} \phi_m(t) + \underbrace{\begin{bmatrix} \frac{K_l(t)K_s}{\rho N_p J_l(t)} \\ 0 \\ 0 \end{bmatrix}}_{\mathcal{G}_s^s(\theta_k)} \phi_m(t) + \underbrace{\begin{bmatrix} \frac{K_l(t)K_s}{\rho N_p J_l(t)} \\ 0 \\ 0 \end{bmatrix}}_{\mathcal{G}_s^s(\theta_k)} \phi_m(t) + \underbrace{\begin{bmatrix} \frac{K_l(t)K_s}{\rho N_p J_l(t)} \\ 0 \\ 0 \end{bmatrix}}_{\mathcal{G}_s^s(\theta_k)} \phi_m(t) + \underbrace{\begin{bmatrix} \frac{K_l(t)K_s}{\rho N_p J_l(t)} \\ 0 \\ 0 \end{bmatrix}}_{\mathcal{G}_s^s(\theta_k)} \phi_m(t) + \underbrace{\begin{bmatrix} \frac{K_l(t)K_s}{\rho N_p J_l(t)} \\ 0 \\ 0 \end{bmatrix}}_{\mathcal{G}_s^s(\theta_k)} \phi_m(t) + \underbrace{\begin{bmatrix} \frac{K_l(t)K_s}{\rho N_p J_l(t)} \\ 0 \\ 0 \end{bmatrix}}_{\mathcal{G}_s^s(\theta_k)} \phi_m(t) + \underbrace{\begin{bmatrix} \frac{K_l(t)K_s}{\rho N_p J_l(t)} \\ 0 \\ 0 \end{bmatrix}}_{\mathcal{G}_s^s(\theta_k)} \phi_m(t) + \underbrace{\begin{bmatrix} \frac{K_l(t)K_s}{\rho N_p J_l(t)} \\ 0 \\ 0 \end{bmatrix}}_{\mathcal{G}_s^s(\theta_k)} \phi_m(t) + \underbrace{\begin{bmatrix} \frac{K_l(t)K_s}{\rho N_p J_l(t)} \\ 0 \\ 0 \end{bmatrix}}_{\mathcal{G}_s^s(\theta_k)} \phi_m(t) + \underbrace{\begin{bmatrix} \frac{K_l(t)K_s}{\rho N_p J_l(t)} \\ 0 \\ 0 \end{bmatrix}}_{\mathcal{G}_s^s(\theta_k)} \phi_m(t) + \underbrace{\begin{bmatrix} \frac{K_l(t)K_s}{\rho N_p J_l(t)} \\ 0 \\ 0 \end{bmatrix}}_{\mathcal{G}_s^s(\theta_k)} \phi_m(t) + \underbrace{\begin{bmatrix} \frac{K_l(t)K_s}{\rho N_p J_l(t)} \\ 0 \\ 0 \end{bmatrix}}_{\mathcal{G}_s^s(\theta_k)} \phi_m(t) + \underbrace{\begin{bmatrix} \frac{K_l(t)K_s}{\rho N_p J_l(t)} \\ 0 \\ 0 \end{bmatrix}}_{\mathcal{G}_s^s(\theta_k)} \phi_m(t) + \underbrace{\begin{bmatrix} \frac{K_l(t)K_s}{\rho N_p J_l(t)} \\ 0 \\ 0 \end{bmatrix}}_{\mathcal{G}_s^s(\theta_k)} \phi_m(t) + \underbrace{\begin{bmatrix} \frac{K_l(t)K_s}{\rho N_p J_l(t)} \\ 0 \\ 0 \end{bmatrix}}_{\mathcal{G}_s^s(\theta_k)} \phi_m(t) + \underbrace{\begin{bmatrix} \frac{K_l(t)K_s}{\rho N_p J_l(t)} \\ 0 \\ 0 \end{bmatrix}}_{\mathcal{G}_s^s(\theta_k)} \phi_m(t) + \underbrace{\begin{bmatrix} \frac{K_l(t)K_s}{\rho N_p J_l(t)} \\ 0 \\ 0 \end{bmatrix}}_{\mathcal{G}_s^s(\theta_k)} \phi_m(t) + \underbrace{\begin{bmatrix} \frac{K_l(t)K_s}{\rho N_p J_l(t)} \\ 0 \\ 0 \end{bmatrix}}_{\mathcal{G}_s^s(\theta_k)} \phi_m(t) + \underbrace{\begin{bmatrix} \frac{K_l(t)K_s}{\rho N_p J_l(t)} \\ 0 \\ 0 \end{bmatrix}}_{\mathcal{G}_s^s(\theta_k)} \phi_m(t) + \underbrace{\begin{bmatrix} \frac{K_l(t)K_s}{\rho N_p J_l(t)} \\ 0 \\ 0 \end{bmatrix}}_{\mathcal{G}_s^s(\theta_k)} \phi_m(t) + \underbrace{\begin{bmatrix} \frac{K_l(t)K_s}{\rho N_p J_l(t)} \\ 0 \\ 0 \end{bmatrix}}_{\mathcal{G}_s^s(\theta_k)} \phi_m(t) + \underbrace{\begin{bmatrix} \frac{K_l(t)K_s}{\rho N_p J_l(t)} \\ 0 \\ 0 \end{bmatrix}}_{\mathcal{G}_s^s(\theta_k)} \phi_m(t) + \underbrace{\begin{bmatrix} \frac{K_l(t)K_s}{\rho N_p J_l(t)} \\ 0 \\ 0 \end{bmatrix}}_{\mathcal{G}_s^s(\theta_k)} \phi_m(t) + \underbrace{\begin{bmatrix} \frac{K_l(t)K_s}{\rho N_p J_l(t)} \\ 0 \\ 0 \end{bmatrix}}_{\mathcal{G}_s^s(\theta_k)} \phi_m(t) + \underbrace{\begin{bmatrix} \frac{K_l(t)K_s}{\rho N_p J_l(t)} \\ 0 \\ 0 \end{bmatrix}}_{\mathcal{G}_s^s(\theta_k)} \phi_m(t) + \underbrace{\begin{bmatrix} \frac{K_l(t)K_s}{\rho N_p J_l(t)} \\ 0 \\ 0 \end{bmatrix}}_{\mathcal{G}_s^s(\theta_k)} \phi_m(t) + \underbrace{\begin{bmatrix} \frac{K_l(t)K_s}{\rho N_p J_l(t)} \\ 0 \\ 0 \end{bmatrix}}_{\mathcal{G}_s^s(\theta_k)} \phi_m(t) + \underbrace{\begin{bmatrix} \frac{K_l(t)K_s}{\rho N_p J_l(t)} \\ 0 \\ 0 \end{bmatrix}}_{\mathcal{G}_s^s(\theta$$

$$\underbrace{\begin{bmatrix} -\frac{C_l(t)}{J_l(t)} & \left(\frac{-K_s}{M_{meq}} - \frac{K_l(t) + K_s \mathcal{J}^2}{J_l(t)}\right) & 0 \\ 1 & 0 & 0 \\ -(K_s \mathcal{J})^{-1} & 0 & 0 \end{bmatrix}}_{\mathcal{F}_a^\delta(\theta_k)} \underbrace{\begin{bmatrix} \dot{F}_s(t) \\ F_s(t) \\ \phi_l(t) \end{bmatrix}}_{x_a(t)}$$

$$+\underbrace{\begin{bmatrix} K_s \\ \rho N_p & \left(\frac{C_l(t)}{J_l(t)} - \frac{B_{meq}}{M_{meq}}\right) + \frac{\rho N_p K_s C_m}{M_{meq}} \\ 0 \\ (\rho N_p \mathcal{J})^{-1} \end{bmatrix}}_{\mathcal{B}_a^{\delta}(\theta_k)} \omega_m(t),$$

$$\underbrace{\begin{bmatrix} \omega_l(t) \\ \phi_l(t) \end{bmatrix}}_{z(t)} = \underbrace{\begin{bmatrix} -(K_s \mathcal{J})^{-1} & 0 & 0 \\ 0 & 0 & 1 \end{bmatrix}}_{C_2} \begin{bmatrix} \dot{F}_s(t) \\ F_s(t) \\ \phi_l(t) \end{bmatrix} + \underbrace{\begin{bmatrix} (\rho N_p \mathcal{J})^{-1} \\ 0 \end{bmatrix}}_{D_2} \omega_m(t), \tag{21}$$

The mechanical impedance of the motor-transmission system has a cartesian inertia  $M_{meq} = \rho^2(J_p + N_p^2 J_m)$ , and damping  $B_{meq} = \rho^2(C_p + N_p^2 C_m)$ ; J and C are the torsional inertia and damping with subscripts m for motor and p for the pulley.  $N_p$  is the pulley ratio and  $\rho$  is a rotational-to-linear factor of ball screw lead. The parameters of the SRPAR are presented in (Jutinico et al., 2017, Table I).

The model consider two operation modes: the active mode,  $\theta_k = 1$ , when the platform torque is opposite to foot torque and the passive mode,  $\theta_k = 2$ , when the platform carries the user's foot. The parameters used for each Markovian

operation mode ( See Table 1) are based on Lee et al. (2016).

Table 1. Nominal human Parameters

Parameter	$\theta_k = 1$	$\theta_k = 2$
$J_h (kg \cdot m^2)$	0.08	0.02
$C_h (N \cdot m \cdot s/rad)$	5	0.5
$K_h (N \cdot m/rad)$	200	20

#### 5.2 Control topology for robust tracking

Control strategy uses an augmented model with integral action and is discretized with a sample time of Ts=2 ms, as follows.

$$\underbrace{\begin{bmatrix} x_{a_{k+1}} \\ x_{int_{k+1}} \end{bmatrix}}_{x_{k+1}} = \underbrace{\begin{bmatrix} F_{a,i} & 0 \\ C_a T_s & 1 \end{bmatrix}}_{F_{i,k}} \underbrace{\begin{bmatrix} x_{a_k} \\ x_{int_k} \end{bmatrix}}_{x_k} + \underbrace{\begin{bmatrix} B_{a,i} \\ 0 \end{bmatrix}}_{B_{i,k}} u_k + \underbrace{\begin{bmatrix} 0 \\ T_s \end{bmatrix}}_{Br_{i,k}} r_k$$
(22)

where  $r_k = F_d$  is a force reference signal and  $C_a = [0 - \dot{1} \ 0]$ .

#### 5.3 Force control design parameters

Table 2 shows the design parameters of LQR-DMJLS force control, and Table 3 shows the control gains for the two Markovian modes.

Table 2. Design Parameters of LQR-DMJLS

$$\begin{bmatrix} Q_{i,k} = \begin{bmatrix} 1 & 0 & 0 & 0 \\ 0 & 250 & 0 & 0 \\ 0 & 0 & 1 & 0 \\ 0 & 0 & 0 & 10 \cdot 10^6 \end{bmatrix}, \ \mathbb{P} = [p_{i,j}] = \begin{bmatrix} 0.6 & 0.4 \\ 0.4 & 0.6 \end{bmatrix}, \\ R_{i,k} = 0.5, \quad P_i(N) = I_4 \cdot 10^{10}, \end{bmatrix}$$

Table 3. Control gains for LQR-DMJLS

Control	$K_1$	$K_2$	$K_3$	$K_{int}$
$\theta = 1$	-0.07	-5.60	-0.33	239.8
$\theta = 2$	-0.04	-2.78	0.18	147.0

The RR-DMJLS uses the same weighting matrices and probability matrix for state transitions that the nominal case. Additionally, the uncertain parameters are shown in Table 4. Table 5 shows the control gains for the two Markovian modes.

Table 4. Design Parameters of RR-DMJLS

Table 5. Control gains for RR-DMJLS

Control	$K_1$	$K_2$	$K_3$	$K_{int}$
$\theta = 1$	-0.01	-8.36	2.18	80.98
$\theta = 2$	-0.03	-3.35	12.81	46.86

#### 6. RESULTS

We generated a set of perturbed markovian plants with one thousand random parameters for each operation mode and calculated the closed-loop system's spectral radius by (19). This random parameters are given by random normally distributed functions,  $\delta J_h \sim N(\mu_{J_h,\theta},\sigma_{J_h,\theta}^2)$ ,  $\delta C_h \sim N(\mu_{C_h,\theta},\sigma_{C_h,\theta}^2)$  and  $\delta K_h \sim N(\mu_{K_h,\theta},\sigma_{K_h,\theta}^2)$ , with the following means and variances,

$$\mu_{J_h,\theta} = J_{h,\theta}, \quad \sigma_{J_h,\theta}^2 = (0.08 \times \mu_{J_h,\theta})^2, 
\mu_{C_h,\theta} = C_{h,\theta}, \quad \sigma_{C_h,\theta}^2 = (0.2 \times \mu_{C_h,\theta})^2, 
\mu_{K_h,\theta} = K_{h,\theta}, \quad \sigma_{K_h,\theta}^2 = (0.2 \times \mu_{K_h,\theta})^2,$$
(23)

where the nominal parameters  $J_{h,\theta}$ ,  $C_{h,\theta}$ , and  $K_{h,\theta}$  were defined in Table 1.

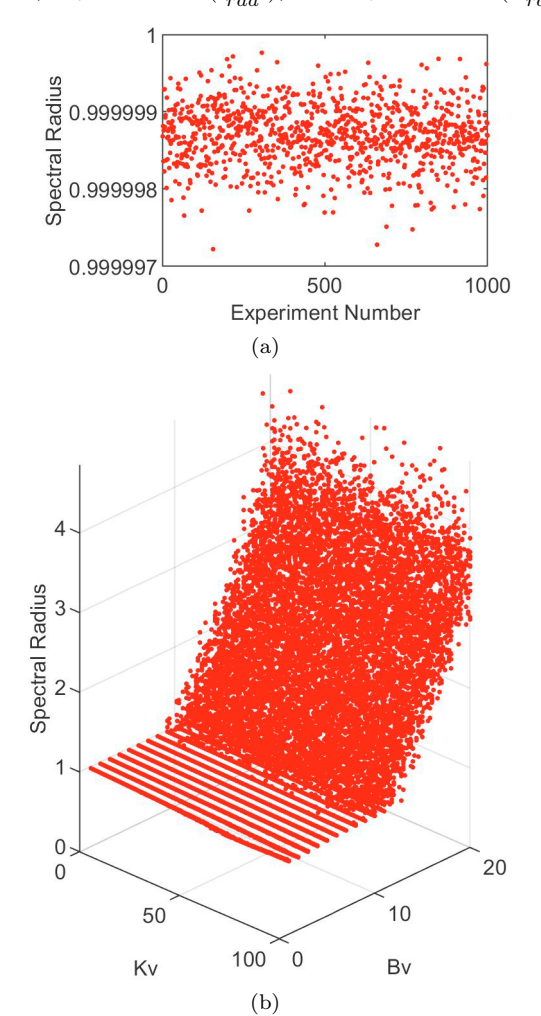
Figure 3 shows the spectral radius calculate when the force control uses the LQR-DMJLS. Notice that spectral radius is less than one for the whole set of plants in the minimal impedance case  $(K_v = 0, B_v = 0)$ , it is to say, the system is mean square stable, as shown in Fig. 3 (a) allowing the system transparency. However, when the impedance is variable the stability is achieved for just 49.16% of tests as shown in Fig. 3 (b). In this case proof rank is  $K_v = [0, 100]$ ,  $B_v = [0, 20]$  and  $\varepsilon = 0.03$ . We highlight that instability occurs for big values of virtual damping  $B_v$ . Figure 4 shows the spectral radius calculate when the force control uses the RR-DMJLS. For this control strategy, mean square stability (MSS) is achieved for the 100% of the tests, both minimal impedance and variable impedance cases. Since the spectral radius is less than one for the whole uncertain set, we affirm that it accomplished robust stability.

#### 6.1 Active and Passive system interaction

To complement the analysis made in this paper, we perform a simulation to show the robot's performance when interacting with the user in both active and passive mode. The test considers the RR-DMJLS and the impedance control with  $K_v=50$  and  $B_v=1$ . Fig. 5 shows in the top the platform torque, in the middle top the load angular position, in the middle bottom the load angular velocity, and the bottom the Markov chain. References signals are depicted in red color and control variables in blue color. Notice that in active mode, the user governs the behavior of the system. Therefore, there are some deviations in  $\phi_l$  and  $\omega_l$ ; in contrast, the platform carries the user's foot in passive mode.

The performance of this system is calculating from the impedance transmissibility from the platform to the user. In this sense, the torque control goal is to track the

Fig. 3. Spectral Radius for IC with LQR-DMJLS. (a) Minimal impedance case. (b) Variable impedance case;  $K_v$  units are  $(\frac{N \cdot m}{rad})$ , and  $B_v$  units are  $(\frac{N \cdot m \cdot s}{rad})$ .



torque reference signal despite human uncertain parameters. From Fig. 5 see that this goal is accomplished with precision. We calculate the root mean square (RMS) value of the actual stiffness  $K_r$  and damping  $B_r$ , using angular velocity and position errors, according to:

$$RMS\{\cdot\} = \sqrt{\frac{1}{N} \sum_{k=1}^{N} \{\cdot\}^2},$$
 (24)

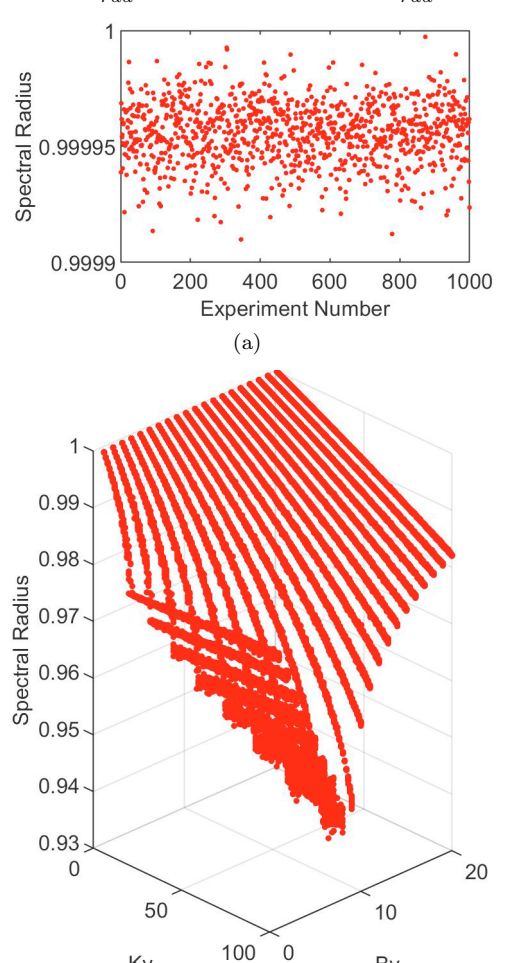
$$K_r = \frac{RMS\{\tau_{K_v}\}}{RMS\{e_{\phi}\}} \text{ and } B_r = \frac{RMS\{\tau_{B_v}\}}{RMS\{e_{\omega}\}}, \qquad (25)$$

where  $\tau_{K_v} = \tau_{plat} - B_v e_\omega$  is the torque generated by the desired stiffness,  $\tau_{B_v} = \tau_{plat} - K_v e_\phi$  is the torque generated by the desired damping, and  $e_\phi = \phi_l^d - \phi_l + \varepsilon \phi_l$  and  $e_\omega = \omega_l^d - \omega_l$  are the angular position and velocity errors, respectively. Obtained results are  $K_r = 49.47$  and Br = 2.97, which shows the high performance given by the impedance control with RR-DMJLS both for active and passive interaction.

#### 7. CONCLUSIONS

In this paper, we show the stability analysis for Markovian interaction systems that use SEA. For this purpose, we

Fig. 4. Spectral Radius IC with RR-DMJLS. (a) Minimal impedance case. (b) Variable impedance case;  $K_v$ units are  $(\frac{N \cdot m}{rad})$ , and  $B_v$  units are  $(\frac{N \cdot m \cdot s}{rad})$ .



made a proof of concept which compares the stability of the SRPAR using an impedance control operating with LQR-DMJLS or RR-DMJLS torque controllers. The former has coupled stability for the nominal case and achieves stability for 49.16% of the tests. The robust approach has complementary stability since it is stable for 100% of the tests. This approach allows designing robots based on SEA considering human parameters, boundary uncertainties, and active and passive user behaviors. Finally, a performance simulation test shows the high impedance transmissibility from the platform to the user, given by the robust control.

(b)

Bv

Κv

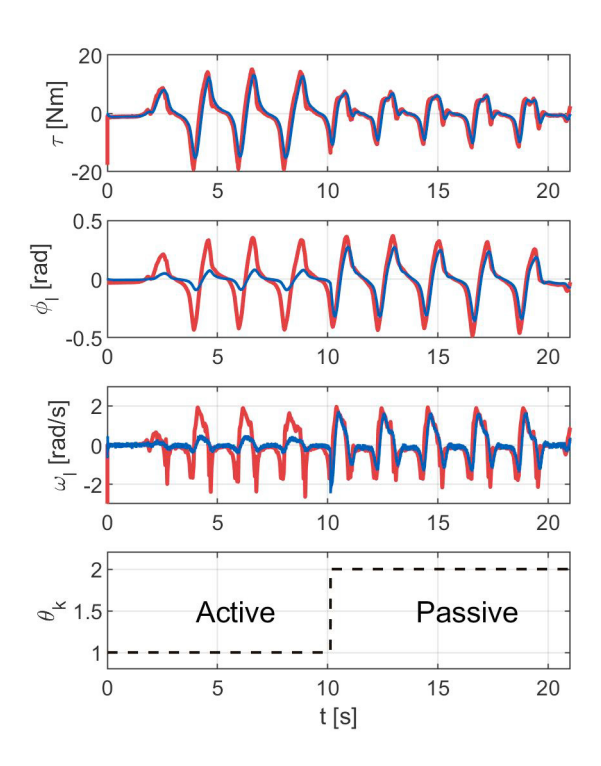
#### ACKNOWLEDGEMENTS

The authors are grateful to the Universidad Distrital Francisco José de Caldas and the University of São Paulo.

#### REFERENCES

Ajoudani, A., Zanchettin, A., Ivaldi, S., Albu-Schäffer, A., Kosuge, K., and Khatib, O. (2018). and prospects of the human-robot collaboration. Au $tonomous\ Robots,\ 42,\ 957-975.$ 

Fig. 5. Test IC with RR-DMJLS,  $K_v = 50$  and  $B_v = 1$ .



Buerger, S.P. and Hogan, N. (2007). Complementary stability and loop shaping for improved human-robot interaction. IEEE Transactions on Robotics, 23(2), 232– 244.

Cerri, J.P. and Terra, M.H. (2017). Recursive robust regulator for discrete-time Markovian jump linear systems. IEEE Transactions on Automatic Control.

Costa, O.L., Fragoso, M.D., and Marques, R. (2005). Discrete-time Markov jump linear systems. Probability and its applications. Springer, London.

Escalante, F.M., Jutinico, A.L., Jaimes, J.C., Terra, M.H., and Siqueira, A.A.G. (2021). Markovian robust filtering and control applied to rehabilitation robotics. IEEE/ASME Transactions on Mechatronics, 26(1), 491–502.

Hogan, N. (1985). Impedance control: an approach to manipulation. Journal of Dynamic Systems, Measurement and Control, 107 (Parts 1-3)(1), 1-24.

Jutinico, A.L., Escalante, F.M., Jaimes, J.C., Terra, M.H., and Siqueira, A.A.G. (2018). Markovian robust compliance control based on electromyographic signals. In 2018 7th IEEE International Conference on Biomedical Robotics and Biomechatronics (Biorob), 1218–1223.

Jutinico, A.L., Jaimes, J.C., Escalante, F.M., Perez-Ibarra, J.C., Terra, M.H., and Siqueira, A.A.G. (2017). Impedance control for robotic rehabilitation: A robust Markovian approach. Frontiers in Neurorobotics, 11, 43.

Lee, H., Rouse, E.J., and Krebs, H.I. (2016). Summary of human ankle mechanical impedance during walking. IEEE Journal of Translational Engineering in Health and Medicine, 4, 1–7.

Pratt, G.A. and Williamson, M.M. (1995). Series elastic actuators. In Proceedings 1995 IEEE/RSJ International Conference on Intelligent Robots and Systems. Human Robot Interaction and Cooperative Robots, 399–406.